UC Davis

Title
Turbulent dispersion via fan-generated flows

Permalink

Journal

ISSN

Authors
Halloran, Siobhan K
Wexler, Anthony S
Ristenpart, William D

Publication Date

DOI

Peer reviewed

Turbulent dispersion via fan-generated flows

Siobhan K. Halloran, Anthony S. Wexler, and William D. Ristenpart

Turbulent dispersion via fan-generated flows

Siobhan K. Halloran,[1] Anthony S. Wexler,[2] and William D. Ristenpart[1,a)]

[1]*Department of Chemical Engineering and Materials Science, University of California Davis, Davis, California 95616, USA*

[2]*Department of Mechanical and Aerospace Engineering, University of California Davis, Davis, California 95616, USA; Air Quality Research Center, University of California Davis, Davis, California 95616, USA; Department of Civil and Environmental Engineering, University of California Davis, Davis, California 95616, USA; and Department of Land, Air and Water Resources, University of California Davis, Davis, California 95616, USA*

Turbulent dispersion of passive scalar quantities has been extensively studied in wind tunnel settings, where the flow is carefully conditioned using flow straighteners and grids. Much less is known about turbulent dispersion in the "unconditioned" flows generated by fans that are ubiquitous in indoor environments, despite the importance of these flows to pathogen and contaminant transport. Here, we demonstrate that a point source of scalars released into an airflow generated by an axial fan yields a plume whose width is invariant with respect to the fan speed. The results point toward a useful simplification in modeling of disease and pollution spread via fan-generated flows. © *2014 AIP Publishing LLC*. [http://dx.doi.org/10.1063/1.4879256]

Turbulent dispersion of passive scalar quantities, like temperature and concentration, has been intensely studied because of the numerous environmental and industrial applications.[1–4] Large-scale studies focusing on dispersion in atmospheric flow conditions are often conducted in the field, where features such as surface roughness and vertical gradients in temperature and wind speed complicate the flow and corresponding interpretation.[5–7] Many dispersion studies have also been performed in more controlled laboratory settings, especially in wind tunnels where the degree of turbulence can be carefully fine-tuned using different control devices: honeycombs straighten the flow and reduce the fan swirl, fine mesh screens suppress the free stream turbulence, and contractions accelerate the flow and make it more isotropic.[8,9] Additionally, fans may be equipped with guide vanes to further ensure that the flow in the test section has minimal swirl.[9–11] The turbulence of interest can then be re-introduced methodically, typically by using a mesh with a coarser size than those used to initially remove the turbulence, yielding nearly isotropic and homogeneous turbulence sufficiently far downstream from the mesh.[12–14] Turbulence generated by grids in this manner was the focus of the seminal studies performed by Taylor and Batchelor,[15–18] and grid-generated turbulence is often used for experiments involving dispersion of scalar quantities, such as temperature,[19,20] particles,[21,22] and dye.[3,23]

In contrast to the flows in wind tunnels, most airflows within indoor environments are not carefully conditioned (i.e., without any flow straightening or other turbulence suppressing features). These "unconditioned" turbulent flows nonetheless play a pivotal role in driving the spread of pathogens and contaminants, and consequently building ventilation and indoor air quality have been the focus of many (primarily computational) studies.[24–26] An important and ubiquitous component of indoor air quality involves the flows generated by basic room fans. In addition to the building ventilation system, fans are often used to increase circulation of stagnant air in indoor spaces, particularly on warm days. However, these fans may also transport unwanted contaminants, such as airborne pathogens expelled by sick individuals and dust accumulated on surfaces, exposing room

---

a)Author to whom correspondence should be addressed. Electronic mail: wdristenpart@ucdavis.edu.

occupants downstream from the fan and contaminant source. While fans are used to generate airflow in wind tunnel experiments, much effort goes toward removing the turbulence they produce, so these flows do not represent the fan-generated turbulence that occurs in a typical indoor environment.

In this work, we consider the short-range dispersion of particulates from a point source located downstream from an axial fan, and we address the question: How does the fan speed affect the turbulent dispersion? A similar question, in the context of mesh-generated turbulence, was addressed nearly a century ago by Taylor.[15,16] In reviewing experimental work by Schubauer[27] on the dispersion of heat in mesh turbulence in a wind tunnel, Taylor noted,[16] ". . . the existing experimental evidence seems to show that turbulent diffusion is proportional to the speed, so that if matter from a concentrated source is diffused over an area downstream from the source, an increase in the speed of the whole system (i.e., proportional increases in turbulent and mean speed) leaves the distribution of matter in space unchanged (though the absolute concentration is reduced)." Thus, an invariance of the passive scalar plume width with the mean background airspeed has been anticipated for later studies with meshes.[23] Here, a single length scale, the mesh size, dictates the turbulence of the flow. However, there is no reason *a priori* that this plume width invariance with mean airspeed should exist for other scenarios, such as dispersion in the atmosphere, where a single length scale tied to turbulence generation cannot be isolated. In addition, for our fan setup, we expect the swirl to contribute angular momentum to the flow, while wind tunnel flows with decaying grid-generated turbulence do not have swirl. Limited studies on axial fan-generated flows in the immediate vicinity of the fan have shown that the flow indeed has a non-zero swirl velocity, and that the turbulence is inhomogeneous and anisotropic.[28,29] However, these studies have only focused on the flow field upstream and in close proximity to the fan. To our knowledge, experiments have not been conducted to characterize the turbulent dispersion of passive scalar quantities further downstream from an axial fan.

Here, we demonstrate experimentally that, for three very different fan configurations, the width of the time-ensemble particulate plume is invariant with the fan speed. We show that while the plume spread does not vary when the speed is adjusted for a single setup, it is affected when the fan configuration is changed, suggesting that the length scale of the fan dictates the turbulence. Additionally, we discuss the implications of our findings for airborne disease transmission between test animals in laboratory settings.

To measure the turbulent dispersivity, we employed a classic technique using tracer smoke particles and a laser sheet[30–32] (Fig. 1(a), Figs. S1(a)–S1(c), Ref. 40). A wire loop (0.33 mm galvanized steel, Hillman), simulating a point source, was coated with 10 cS poly(dimethylsiloxane) fluid (Sigma Aldrich) and connected to a 3 A power supply (PR3-UL, Tripp Lite). The oil was heated to its smoke point when the power supply was switched on. The generated smoke was transported downstream by one of three fan setups: a 50.8 cm box fan (Lasko, Fig. 1(b)), a 25.4 cm circular fan (Honeywell Power Air Circulator, Fig. 1(c)), or a 4×7 configuration of 8 cm low speed CPU fans (Evercool, Fig. 1(d)). The front grills were removed from the box fan and circular fan; the CPU fans did not have grills. To minimize possible disturbances from other airflow sources in the laboratory, all experiments were conducted in a $67 \times 33 \times 55$ cm acrylic box, with the front and rear sides removed to allow the fan-generated airflow to pass through. Experiments with and without the
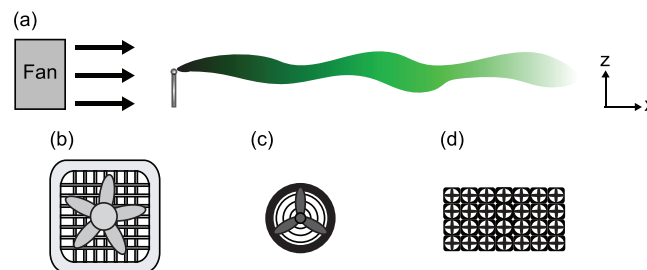

FIG. 1. (a) Schematic of laser dispersivity experimental setup. Silicone oil smoke is dispersed from a simulated point source in flow generated by a (b) box fan, (c) circular fan, or (d) fan array. The smoke particulates are visualized using a laser sheet from above (not shown). See Fig. S1 (Ref. 40) for details.

box demonstrated the box walls had no appreciable effect on the measured plume widths (cf. Fig. S2, Ref. 40). The point source was approximately centered vertically ($\sim$16.5 cm from the bottom and top of the box) and depth wise ($\sim$27.5 cm from the back and front of the box), and was about 20 cm downstream from the box inlet. The circular and box fans were both placed about 90 cm upstream of the box opening, while the fan array was attached directly to the inlet of the box. The mean background airspeed, U, varied for each setup: For the box fan, U ranged from 104 to 170 cm/s, for the circular fan, U ranged from 140 to 207 cm/s, and for the fan array, U ranged from 40 to 100 cm/s ($Re_{fan} \approx 10^4$, defined for the average characteristic length scale of the fans). The fan speeds for the box and circular fans were adjusted using the built-in controls, which allowed for three speeds for each fan. The fan array speed was controlled via pulse width modulation using a solid-state relay (Kyoto Electric KG 1010D) and a data acquisition card with Labview software (National Instruments). The airspeed was measured downstream from the wire at the outlet of the acrylic box using a hot-wire anemometer (Alnor Velometer Thermal Anemometer AVM 410, TSI).

As the smoke was transported downstream, it was illuminated by a laser sheet, generated using a 150 mW 532 nm green DPSS laser (GML series, Lasermate) and a 75° fan angle laser line generator (Laserline Optics Canada), suspended over the box. The smoke plume progression was recorded using high-speed video (Phantom v 7.3) with a frame rate of 50 images per second. Images were thresholded and integrated using standard image analysis techniques in Matlab.

Fig. 2(a) shows a representative snapshot of the particulate plume. The instantaneous plume appears randomly distributed by the turbulent airflow generated by the fan. In contrast, the time-integrated plume is more orderly. Fig. 2(b) shows a contour plot of the integrated particulate intensity over 100 s, where the instantaneous particulate intensities (in arbitrary units) have been integrated
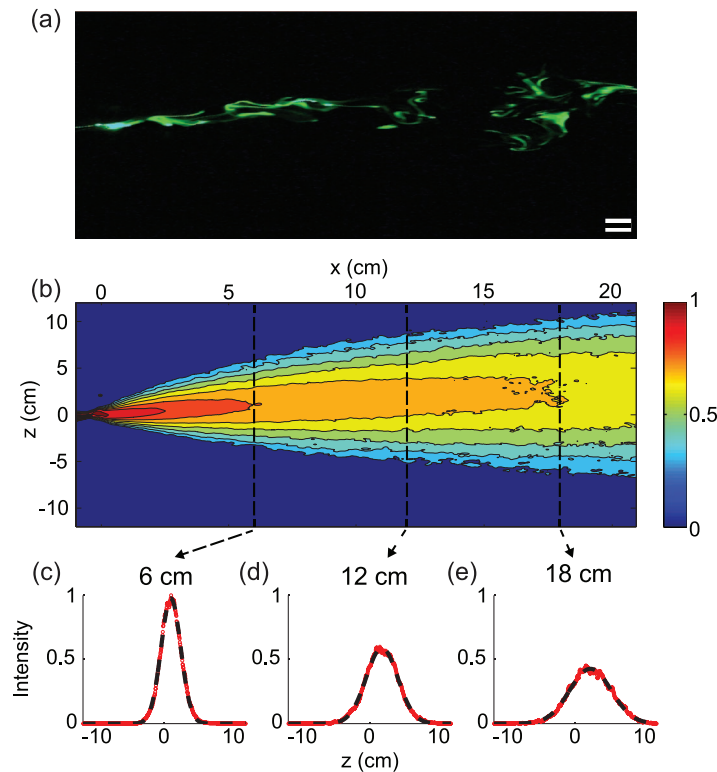

FIG. 2. Representative particulate dispersion for the fan array. (a) Typical experimental image of the instantaneous particulate distribution as illuminated by the laser sheet. Scale bar is 1 cm. (b) Contour plot of the time integrated particulate intensity (I, arbitrary units) for one experimental trial of duration 100 s. Contours shown as $\log(I)/\log(I_{max})$; red denotes high particulate concentration, blue denotes zero concentration. (c)–(e) Cross sectional profiles of normalized particulate intensity vs. vertical displacement. Red markers: experimental measurements; black dashed lines: Gaussian distributions fit via nonlinear regression.

and normalized on a logarithmic scale to indicate the time ensemble plume behavior. Qualitatively, the plumes display the expected behavior: smoke is highly concentrated close to the point source, and spreads in the cross-flow direction via turbulent dispersion as it is transported downstream.

For homogeneous and isotropic turbulence, the turbulent dispersivity in the directions perpendicular to the mean flow can be calculated by fitting the observed time-averaged particulate concentration versus the cross-flow coordinate at a fixed downstream position to a Gaussian profile;[12] the dispersivity σ_z is the width parameter extracted from the fit (i.e., the standard deviation). Note that this procedure does not depend on the absolute particulate concentration, since it yields only the plume width. Although it was not clear *a priori* that the fans would yield homogenous and isotropic turbulence, the time-averaged concentration profiles in the plumes were nonetheless Gaussian. Figs. 2(c)–2(e) show the particulate distribution for three representative positions downstream, and it is clear that the corresponding Gaussian fits (black dashed lines) represent the concentration profiles to excellent approximation. The dispersivity values for the Gaussian plots shown in Figs. 2(c)–2(e) are $\sigma_z = 1.45 \pm .01$ cm, $\sigma_z = 2.34 \pm .01$ cm, and $\sigma_z = 3.07 \pm .02$ cm, respectively, where the error reported is the 95% confidence interval for the fit. In addition to reporting this confidence interval, we also performed a consistency check on the dispersivity calculations, varying the number of frames analyzed. Qualitatively similar plumes were observed with all three fan configurations.

Parallels can be drawn between the spread of smoke particles in a turbulent fan-generated flow and the spread of momentum in a round jet. As demonstrated by Fig. 3, the smoke particulate intensity profiles are self-similar; for varied positions downstream from the wire, the particulate intensities, normalized by the maximum intensity, collapse when plotted against the z-coordinate, normalized by the dispersivity. A similar collapse is expected for the velocity profiles in a self-similar jet.[33,34]

The plume widths as measured via the procedure outlined in Fig. 2 are plotted versus downstream position in Fig. 4. The dispersivity is consistently largest for the box fan (Fig. 4(a)), which has the largest blade chord of any of the fans. This fan also yields dispersivities with the highest variability, conceivably a result of the large degree of turbulence kinetic energy in this flow. The calculated dispersivities are more similar for the circular fan and the fan array (Figs. 4(b) and 4(c)), likely due to the comparable length scales of the fan configurations. Initially, all fan setups appear to yield dispersivities that vary linearly with downstream position, following Taylor's[15] predictions for the near field spread from a point source in homogeneous, isotropic turbulence.

The key observation is that for a given fan configuration, the plume spread was insensitive to the imposed airspeed. Increases in airspeed of 63% for the box fan, 48% for the circular fan, and 150% for the fan array all had no significant impact on the respective plume width. To ensure that the source strength was not having an effect on the calculated dispersivity, additional experiments were performed with a smaller quantity of tracer smoke. These tests again confirmed that the plume spread
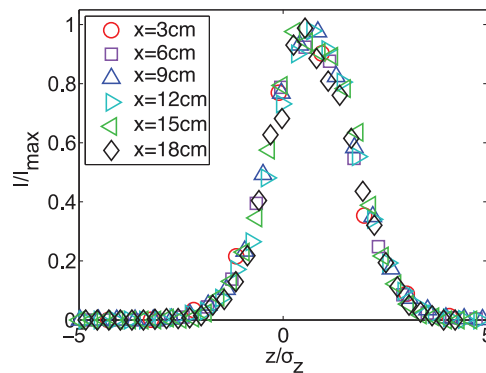

FIG. 3. Normalized particulate intensity, I/I_{max}, vs. normalized z-coordinate, z/σ_z, for fixed downstream positions for experiments with the fan array. Note that within the range of measured conditions the distribution of smoke in the cross-flow direction is self-similar.
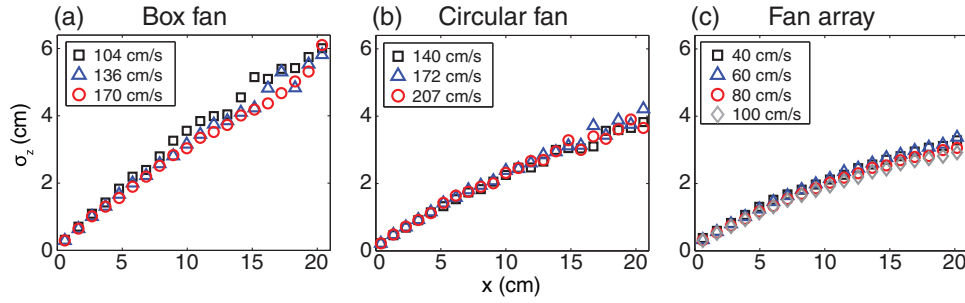
FIG. 4. Particulate plume widths, as characterized by the dispersivity σ_z, versus downstream position for varied air speeds and fan configurations: (a) box fan, (b) circular fan, (c) fan array. Assuming an error of ± 1 pixel, our error is too small to plot. Each σ_z was found via nonlinear regression of the Gaussian distribution against the observed intensity profiles, typified by those shown in Figs. 2(c)–2(e). Note that for a given fan configuration the plume width is insensitive to the air speed.

is invariant with the mean background airspeed. As mentioned above, qualitatively similar invariance of the plume width with mean velocity has been demonstrated for mesh-generated turbulence.[19,23,27] Additionally, it has been shown for other carefully "conditioned" flows, such as fully developed pipe flow.[30] However, to our knowledge this velocity-independent plume width has not been reported for unconditioned flow downstream from a fan.

The plume width independence of fan speed indicates that the effective turbulent diffusivity, which controls the particulate spread normal to the flow direction, scales directly with the fan speed. This behavior can be rationalized in terms of a convective-diffusive scaling analysis. In conditions where flow downstream is dominated by the mean background velocity (i.e., $U \gg u_x$), transport via turbulent diffusion is primarily in the cross-flow directions. Thus, for our experiments, the convection-diffusion equation simplifies to $U \frac{dC}{dx} = D_T \frac{d^2C}{dz^2}$, where D_T is the turbulent diffusivity (assumed to be much greater than the molecular diffusivity). Following the classic interpretation,[8,35] the turbulent diffusivity scales as $D_T \sim u_z l_f$ where u_z is a characteristic turbulent velocity (in this case induced by the fan), and l_f is a mixing length which we assume is the characteristic length scale of the fan. For the box fan and circular fan, we use the fan blade chord as the characteristic length scale, 18 and 9 cm, respectively. For the fan array, we use the diameter of a single entire fan instead, 8 cm, assuming this is the mixing length for this multi-fan arrangement. Choosing the plume width, σ_z, as the characteristic z length scale and substituting into the convection-diffusion equation yields the scaling estimate,

$$\sigma_z \sim \sqrt{\frac{u_z}{U} l_f x}. \tag{1}$$

Since our observed plume widths are insensitive to U (cf. Fig. 4), the key implication of Eq. (1) is that the turbulence intensity i_z is constant for a particular fan setup, i.e., $i_z = \frac{u_z}{U} = k$, and the turbulent velocity scales directly with the mean velocity. Fig. 5 illustrates a dimensionless form of the scaling analysis. The dispersivities for each fan were averaged across the fan speeds tested. Since we did not directly measure the turbulence intensity, i_z was fit via linear interpolation of the dispersivity approaching the origin, assuming Taylor's[15] near field theorem was valid in this region. The estimated turbulence intensities were 0.33, 0.23, and 0.20 for the box fan, circular fan, and fan array, respectively. Both axes were nondimensionalized using the characteristic length scale of the fan, l_f. Fig. 5 demonstrates that the scaling for the average dispersivities of the three experimental fan configurations all fall onto a single curve. The dependence of the dispersivity on the square root of downstream displacement in Eq. (1) is expected for the far field in homogeneous and isotropic turbulent flows.[15] While the near field dispersivity is instead expected to vary linearly with position, Fig. 5 shows that Eq. (1) provides a reasonable approximation over the range of measured conditions. Since the characteristic length scale for the box fan is the largest, the data points for this fan are clustered closest to the origin, while the data points for the fan grid, with the smallest characteristic length scale, extend furthest downstream. Fig. 5 confirms that it is the length
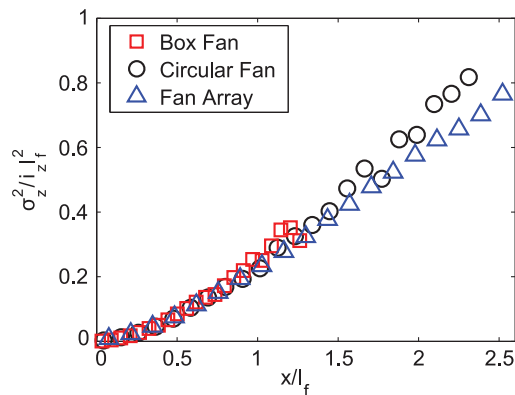
FIG. 5. Dimensionless scaling analysis for the fan-generated turbulence. The square of the turbulent dispersivity σ_z is normalized by the turbulence intensity i_z and the square of the characteristic length scale of the fan l_f. Distance downstream from the wire x is also normalized by l_f.

scale of each fan, not the fan speed that is dictating the turbulence and thus the passive scalar plume spread.

In summary, the answer to our initial question – how does the fan speed affect the turbulent dispersion in the cross-flow directions? – is simply, "It does not." The turbulence intensity generated by three very different fan configurations was insensitive to the fan speed, yielding plume development one would expect for homogenous and isotropic turbulence despite the lack of any preconditioning via flow straightening or turbulence suppressing devices. Interestingly, our findings for passive scalar dispersion in swirling fan-generated turbulent flows mirror the results expected for swirl-free flows with grid-generated turbulence. While unregulated flows have been rigorously studied for larger scale applications for atmospheric dispersion, to our knowledge they have not been previously examined for the fan generated, small-scale flows used in our experiments and common in numerous residential, commercial, and laboratory situations. Thus, with this "fan generated turbulence," changing the fan configuration (i.e., its geometry), not the fan speed, alters the plume spread. Although here we focused on the cross-flow dispersion, in the future, this study can be extended to consider the turbulence in the direction of the mean flow as well.

An important implication of our results is interpretation of experiments focusing on airborne disease transmission between laboratory animals, which often involve fans moving air past a purposely inoculated animal toward a test animal. We recently presented a model predicting the probability of airborne disease transmission in a turbulent flow between test animals.[36] In these experiments, the fluid mechanics have not been explicitly considered, and the fan configuration often varies between labs.[37–39] There is no control of the flow, but the turbulence intensity presumably affects the dispersal of expelled respiratory particles and thus the likelihood of transmission. Our results here indicate that the width of the expiratory droplet plume will not be affected by changes in the fan speed, although the concentration magnitude downstream will definitely depend on the speed due to dilution of the source by the larger airflow. Our findings instead indicate the pathogen plume width will be affected by different fan configurations. Careful consideration should be given to the source of the airflow when considering pathogen or contaminant transmission in laboratory conditions.

[1] R. J. Brown and R. W. Bilger, "An experimental study of a reactive plume in grid turbulence," J. Fluid Mech. **312**, 373 (1996).

[2] B. I. Shraiman and E. D. Siggia, "Scalar turbulence," Nature (London) **405**, 639 (2000).

[3] A. C. Rummel, S. A. Socolofsky, C. F. Von Carmer, and G. H. Jirka, "Enhanced diffusion from a continuous point source in shallow free-surface flow with grid turbulence," Phys. Fluids **17**, 075105 (2005).

[4] L. Sabban and R. van Hout, "Measurements of pollen grain dispersal in still air and stationary, near homogeneous, isotropic turbulence," J. Aerosol Sci. **42**, 867 (2011).

[5] W. W. Kellogg, "Diffusion of smoke in the stratosphere," J. Meteorol. **13**, 241 (1956).

[6] P. R. Slawson and G. T. Csanady, "The effect of atmospheric conditions on plume rise," J. Fluid Mech. **47**, 33 (1971).

[7] G. T. Csanady, *Turbulent Diffusion in the Environment* (D. Reidel Publishing Company, Boston, 1973).

[8] G. Comte-Bellot and S. Corrsin, "The use of a contraction to improve isotropy of grid-generated turbulence," J. Fluid Mech. **25**, 657 (1966).

[9] J. B. Barlow, W. H. Rae, and A. Pope, *Low-Speed Wind Tunnel Testing* (John Wiley and Sons, New York, NY, 1999).

[10] P. Bradshaw and R. C. Pankhurst, "The design of low-speed wind tunnels," Prog. Aerosp. Sci. **5**, 1 (1964).

[11] J. Groth and A. V. Johansson, "Turbulence reduction by screens," J. Fluid Mech. **197**, 139 (1988).

[12] J. O. Hinze, *Turbulence* (McGraw-Hill, New York, 1975).

[13] E. M. Laws and J. L. Livesey, "Flow through screens," Annu. Rev. Fluid Mech. **10**, 247 (1978).

[14] S. B. Pope, "Simple models of turbulent flows," Phys. Fluids **23**, 011301 (2011).

[15] G. I. Taylor, "Diffusion by continuous movements," Proc. London Math. Soc. **s2–20**, 196 (1922).

[16] G. I. Taylor, "Statistical theory of turbulence," Proc. R. Soc. London, Ser. A **151**, 421 (1935).

[17] G. K. Batchelor and A. A. Townsend, "Decay of isotropic turbulence in the initial period," Proc. R. Soc. London, Ser. A **193**, 539 (1948).

[18] G. K. Batchelor and A. A. Townsend, "Decay of turbulence in the final period," Proc. R. Soc. London, Ser. A **194**, 527 (1948).

[19] M. S. Uberoi and S. Corrsin, "Diffusion of heat from a line source in isotropic turbulence," NACA Report No. 1142, 1953.

[20] A. A. Townsend, "The diffusion behind a line source in homogeneous turbulence," Proc. R. Soc. London, Ser. A **224**, 487 (1954).

[21] W. H. Snyder and J. L. Lumley, "Some measurements of particle velocity autocorrelation functions in a turbulent flow," J. Fluid Mech. **48**, 41 (1971).

[22] M. R. Wells and D. E. Stock, "The effects of crossing trajectories on the dispersion of particles in a turbulent-flow," J. Fluid Mech. **136**, 31 (1983).

[23] R. E. Britter, J. C. R. Hunt, G. L. Marsh, and W. H. Snyder, "The effects of stable stratification on turbulent-diffusion and the decay of grid turbulence," J. Fluid Mech. **127**, 27 (1983).

[24] W. Lu and A. T. Howarth, "Numerical analysis of indoor aerosol particle deposition and distribution in two-zone ventilation system," Build. Environ. **31**, 41 (1996).

[25] H. Xing, A. Hatton, and H. B. Awbi, "A study of the air quality in the breathing zone in a room with displacement ventilation," Build Environ. **36**, 809 (2001).

[26] P. V. Nielsen, Y. G. Li, M. Buus, and F. V. Winther, "Risk of cross-infection in a hospital ward with downward ventilation," Build. Environ. **45**, 2008 (2010).

[27] G. B. Schubauer, "A turbulence indicator utilizing the diffusion of heat," NACA Report No. 524, 1935.

[28] J. M. F. Oro, K. M. A. Diaz, C. S. Morros, and E. B. Marigorta, "Unsteady flow and wake transport in a low-speed axial fan with inlet guide vanes," J. Fluids Eng. **129**, 1015 (2007).

[29] J. M. F. Oro, K. M. A. Diaz, C. S. Morros, and E. B. Marigorta, "On the structure of turbulence in a low-speed axial fan with inlet guide vanes," Exp. Therm. Fluid Sci. **32**, 316 (2007).

[30] H. A. Becker, R. E. Rosensweig, and J. R. Gwozdz, "Turbulent dispersion in a pipe flow," AIChE J. **12**, 964 (1966).

[31] M. Gad-el-Hak and J. B. Morton, "Experiments on the diffusion of smoke in isotropic turbulent-flow," AIAA J. **17**, 558 (1979).

[32] D. S. Hui, S. D. Hall, M. T. V. Chan, B. K. Chow, J. Y. Tsou, G. M. Joynt, C. E. Sullivan, and J. J. Y. Sung, "Noninvasive positive-pressure ventilation - An experimental model to assess air and particle dispersion," Chest **130**, 730 (2006).

[33] I. Wygnanski and H. Fiedler, "Some measurements in self-preserving jet," J. Fluid Mech. **38**, 577 (1969).

[34] S. B. Pope, *Turbulent Flows* (Cambridge University Press, Cambridge, 2000).

[35] P. A. Davidson, *Turbulence: An Introduction for Scientists and Engineers* (Oxford University Press, New York, 2004).

[36] S. K. Halloran, A. S. Wexler, and W. D. Ristenpart, "A comprehensive breath plume model for disease transmission via expiratory aerosols," PLoS ONE **7**, e37088 (2012).

[37] A. C. Lowen, S. Mubareka, J. Steel, and P. Palese, "Influenza virus transmission is dependent on relative humidity and temperature," PLoS Pathog. **3**, e151 (2007).

[38] S. Herfst, E. J. A. Schrauwen, M. Linster, S. Chutinimitkul, E. de Wit, V. J. Munster, E. M. Sorrell, T. M. Bestebroer, D. F. Burke, D. J. Smith, G. F. Rimmelzwaan, A. D. M. E. Osterhaus, and R. A. M. Fouchier, "Airborne transmission of influenza A/H5N1 virus between ferrets," Science **336**, 1534 (2012).

[39] S. Herfst, E. J. Schrauwen, M. Linster, S. Chutinimitkul, E. de Wit, V. J. Munster, E. M. Sorrell, T. M. Bestebroer, D. F. Burke, D. J. Smith, G. F. Rimmelzwaan, A. D. Osterhaus, and R. A. Fouchier, "Airborne transmission of influenza A/H5N1 virus between ferrets," Science **336**, 1534 (2012).

[40] See supplementary material at http://dx.doi.org/10.1063/1.4879256 for figures showing detailed schematics of the experimental setup and a comparison of calculated dispersivities with and without the box present for the circular fan.